Anais XIII Simpósio Brasileiro de Sensoriamento Remoto, Florianópolis, Brasil, 21-26 abril 2007, INPE, p. 5011-5018.

Use of multi-polarization L-band R99SAR for coastal wetland zone recognition in the Amazon Region

Pedro Walfir Martins Souza Filho
Francisco Ribeiro da Costa
Fabrício Dias Gonçalves

Laboratório de Análise de Imagens do Trópico Úmido,
Centro de Geociências, Universidade Federal do Pará,
Caixa Postal 8608 - 66075-110, Belém -PA, Brasil. {walfir, frc, fdias}@ufpa.br

Abstract. The purpose of this study was to assess the use of multi-polarization L-band R99SAR for identification of different coastal wetland environments in the Bragança coastal plain in northern Brazil. The information extraction was based on recognition of the mechanism interactions occurring between radar signal and the target on the ground, represented by shallow water morphology in the intertidal conditions, coastal dunes, mangroves, marshes and highland. The results showed that VV-polarization is the best to recognize intertidal morphology under low spring tide conditions. On the other hand, HH-polarization showed to be better to map coastal environments covered by forest and scrub vegetation, such as mangrove and vegetated dunes, respectively, while, HV-polarization is the best to distinguish the contact between transitional zones (e.g. mangrove and coastal plateau). Therefore, high-resolution SAR R99B data can provide an excellent source for identification and delineation of geomorphic targets in the wetlands zones.

Palavras-chave: Mapsar, L-band, mangrove, Amazon, coastal mapping, banda L, manguezal, Amazônia, coastal mapping.

1. Introduction

Different authors have showed that present orbital SAR and optical data proved to be a fundamental source of information for both geomorphologic mapping and monitoring coastal changes in the wetland zones (Parmuchi et al., 2002; Souza Filho and Paradella, 2005; Souza Filho et al., 2006). Recent studies have addressed the use of orbital Synthetic Aperture Radar (SAR) as an ideal data source for flooding, wetland and hydrological studies in the Amazon (Mougin et al. 1999, Proisy et al., 2000; Costa et al. 2002). The cloud penetration ability and the day/night imaging capabilities allow valuable information to be extracted when data acquired by conventional optical remote sensing imagery are restricted.

In wetland zones, under mangrove forested canopies there is water over the ground layer. This is responsible for significant increase in ground-trunk two-double bounce scattering, which in turn, results in an increase in radar backscatter (Kasischke et al., 1997). According Hess et al. (1990), the ground-trunk scattering is typically detected using only longer wavelength (L- and P-bands). On the other hand, in fresh and brackish marshes, the double-bounce mechanism is a response of water-leaves scattering produced over flooded grasslands. Pope et al. (1997) observed that L-HH is the optimum single-frequency and polarization to flood detection in marsh areas.

This paper demonstrate the use of multi-polarized L-band SAR R99B data within selected coastal wetlands application. First application includes the recognizing of different wetland environments (e.g. mangrove and marsh). Second, emphasize the use of multipolarization to distinguish various geomorphic targets in the intertidal zone.

2. Study Area

The test site is represented by the Bragança coastal plain, which is located in a large macrotidal mangrove coast in the northern Brazil (**Figure 1**). This area is an extensive (more

than 20 km wide) and low gradient intertidal zone available for mangrove colonization that forms a fringe wetland vegetation zone between coastal plateaus and the sea (Souza Filho et al. 2006). Mangrove vegetation is composed of forests with trees reaching up to 20 m in height and brackish or marine waters as a result of tidal action that regularly overflow them.

The intertidal sandflat are wide and become completely exposed during the low tide. Strong bi-directional tidal currents characterize the Caeté Estuary and other tidal channels, which has a funnel-shaped mouth, straight and meandering segments and up-stream tidal channel (Souza Filho and Paradella, 2002).

The area is subject to a hot and humid equatorial climate, with well-defined dry (September to December) and wet (January to August) seasons and an annual average precipitation around 2,550 mm. The study area is a tide-dominated setting characterized by a semidiurnal macrotidal regime. The digital integration of RADARSAT Fine 1 and Landsat TM data allows the recognition of nineteen geobotanical units in the Bragança coastal plain, as presented in **Figure 1**. (Souza Filho and Paradella, 2002).

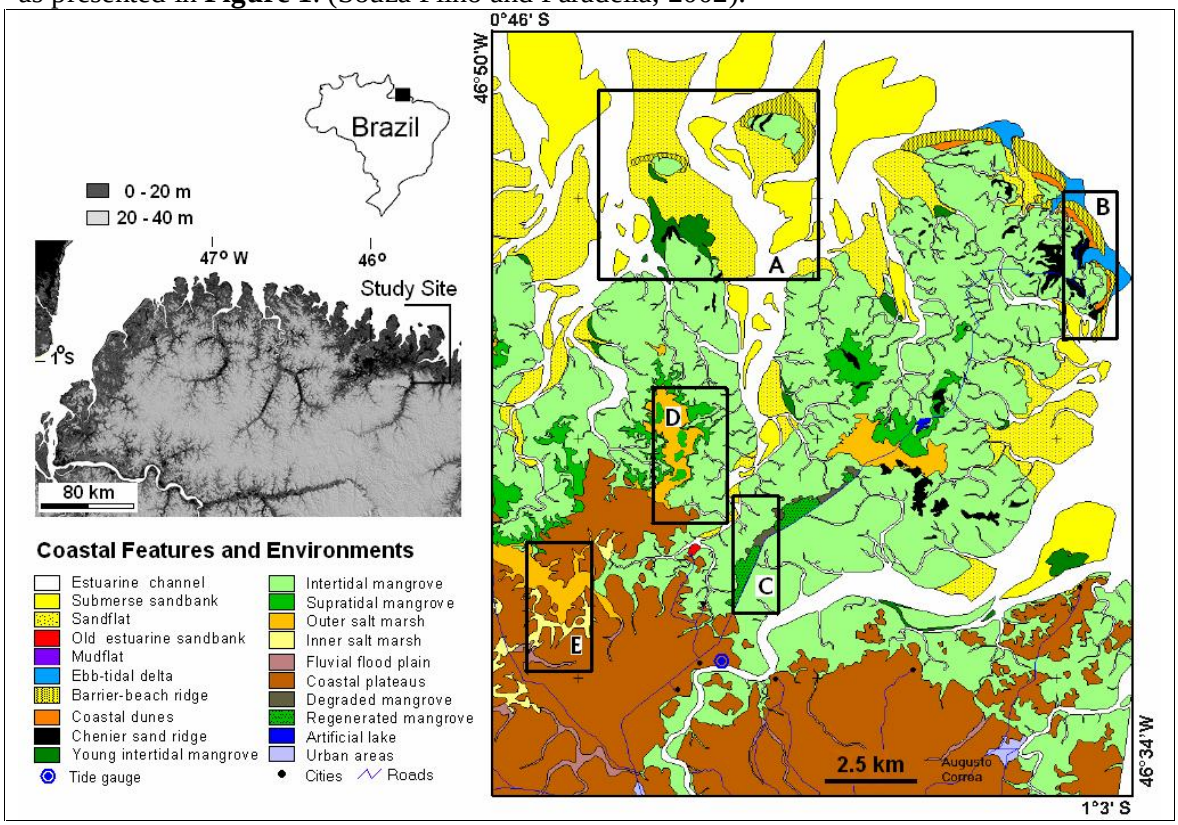

Figure 1. Location of study area. Six distinct regions are identified over geomorphological map (Souza Filho and Paradella, 2002). A) Taperaçu intertidal sandflat, B) Ajuruteua macrotidal beach and coastal dunes, C) Intertidal mangrove areas, D) and E) Supratidal mangroves, marshes and coastal plateau – transitional zone.

3. Methodology

SAR R99B image acquisition and MAPSAR simulation

In this study we use L-band multi-polarization SAR imagery collected aboard Amazon Surveillance System's (SIVAM) EMB-145 aircraft, with SAR R99B sensor. This mission was carried out by National Institute for Space Research (INPE) and Deutschen Zentrums für Luft- und Raumfahrt (DLR) for simulate Multi-Application Purpose SAR (MAPSAR)

images. This study has been conducted as an analog for future high resolution and polarimetric small satellite, such as MAPSAR.

Multi-polarization L-band image was acquired using a NNE-SSW flight path with a swath width of 20 km and 6 m of ground spatial resolution. The incident angle ranges from 39,57^o in the near-range to 70,99^o in the far-range. These strips were used to generate a mosaic to simulate MAPSAR image. Considering this initiative, eleven strips were processed in the Regional Surveillance Center (CRV) at CENSIPAM (System for the Protection of the Amazon Region), using PROSAR (SAR Processor) system, developed by Aeronautic Technological Center (CTA). The strips were geometrically co-registered and joined together to be generated a mosaic. As the MAPSAR data in the Medium Resolution Mode presents 10 m of spatial resolutions, and incident angle ranges from 20^o to 48.1^o (Schröder et al. 2005), the resolution of the mosaic was resampled to 10 m, and it was only used the incident angle interval from 45^o to 53^o of each strip used in this simulated data. Hence, SAR images mosaics of L-band in different polarizations (HH, VV and HV) were produced. The histograms of HH, VV and HV mosaics were equalized (Mura et al., 2006). It is important to point out that differences observed between strips are related to joint position of pixels with distinct incidence angle and signal-noise relation. These differences are more evinced in the HV polarization due to smaller response of the targets in this polarization.

Field methods

On May 24, 2006, eleven strips of data were captured from 13:21 to 17:40 pm under low spring tide water condition (**Figure 2**).

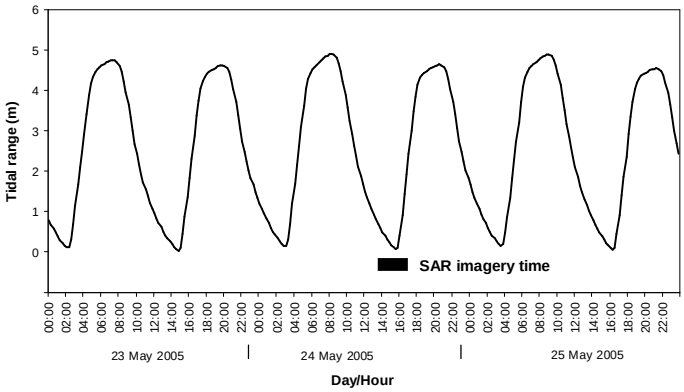

Figure 2. Time series plot of the tidal range during acquisition of SAR image in Caeté estuary. See the location of tide-gauge in Figure 1.

Before radar acquisition, ground data were collected on an extensive fieldwork campaigns in order to identify areas of interest to check the features observed in the image interpretation. In this way, RADARSAT Fine 1 and Landsat TM 5 images were used to discriminate the various tidal sub-environments (Souza Filho and Paradella, 2002). Field observations were made simultaneously to SAR image acquisition (20-27 May 2005). After SAR R99B acquisition, a geomorphological mapping were carried out to identified vegetation, sediment texture and landforms of different coastal units, which were positioned through of global positional system (GPS).

Data processing and analysis

In order to reduce speckle, one of the main problems when dealing with SAR digital data, the adaptive enhanced-Frost filter (3x3 window) was used. The image was linearly stretched in

order to enhance contrasts between the coastal features, and visually interpreted based on conventional photointerpretation keys (tone, texture, pattern, form, size and context). Oblique air-photos were also used as ancillary data during the interpretation and ground truth data were acquired during the field work. The coastal features were analyzed based on multi-polarization response.

4. Results

Image analysis consisted of visual interpretation of the L-band multi-polarization amplitude images and the composite image. Six distinct regions are shown over geomorphological map (Souza Filho and Paradella, 2002) in Figure 1. They are: A) Taperaçu intertidal sandflat, B) Ajuruteua macrotidal beach and coastal dunes, C) Intertidal mangrove areas, D) and E) Supratidal mangroves, marshes and coastal plateau – transitional zone.

Taperaçu intertidal sandflat

In the mouth of Taperaçu estuary occurs one large intertidal sandflat (Figure 1). This intertidal sandflat occurs along the coast between mean tidal and low spring tidal levels. Sandy tidal shoals with abundant linguoid ripples (0.05 m in height and 0,3 m in wavelength), sinuous and linear megaripples (0.5 m in height and 10 m in wavelength), and plane beds are exposed at low tide (Souza Filho and El-Robrini, 2000).

Figure 3 shows the three polarizations and a composite image of the Taperaçu intertidal sandflat. Comparison of the three individual polarization amplitude images indicates some differences in the terrain response. Bedform structures are well pronounced only in VV-polarization. It provides a better discrimination of the large bedforms than megaripples superinmposed to sandbars in response to vertically transmited electric vector couples more effectively than HH to the vertical changes of the bedforms. The contrast between well-defined bright (tidal channels, megariples and man-made structures) and dark region (plane bed forms over sand bars) in the VV-polarizations reveals the shallow water morphology of the intertidal sandflat.

In comparison , the HH-polarization image reveals only man-made structures to catch fish trap located over sandy bars. As well as HV-polarization, HH-polarization reveals nothing in relation to sand bars and its megaripples superimposed, and shallow water morphology. The composite images reveals that VV-polarization is capable of recognizing shallow water morphology (in blue color), while man-made structure is perceptible in HH- and VV-polarization (in magenta color).

Ajuruteua macrotidal beach and coastal dunes

Sandy sediments of intertidal sandflat are reworked by the wind to constitute the coastal sandy dunes, which are currently migrating landward over the mangrove deposits in the intertidal mudflats. Transverse dunes are composed of well-sorted and very fine quartz sands and are partially or completely covered by vegetation. Three different generations of coastal vegetated dunes can be observed in the study site. The beach ridges extend from the low spring tidal levels to coastal dune-beach scarps that represent the higher spring tidal level in the intertidal beach. The beaches have a linear and elongated form along an east-west direction, with curved spits in the longshore sediment transport direction (Souza Filho and El-Robrini, 2000).

A composite image and three-polarization amplitude images are shown in **Figure 3**. The composite image shows that the SAR R99B image is capable of recognizing intertidal zone of the macrotidal beach and the main coastal dunes sub-environment. Distinction can be made

between vegetated dunes and salty sandflat. The intertidal zone of the Ajuruteua macrotidal beach can be identified only in VV-polarization. It appears like a very smooth and dark surface in response L-band interaction with plane bedforms, in contrast to interaction with brag-waves in the nearshore zone. In the HH- and HV-polarization the intertidal beach zone has the same response of nearshore zone.

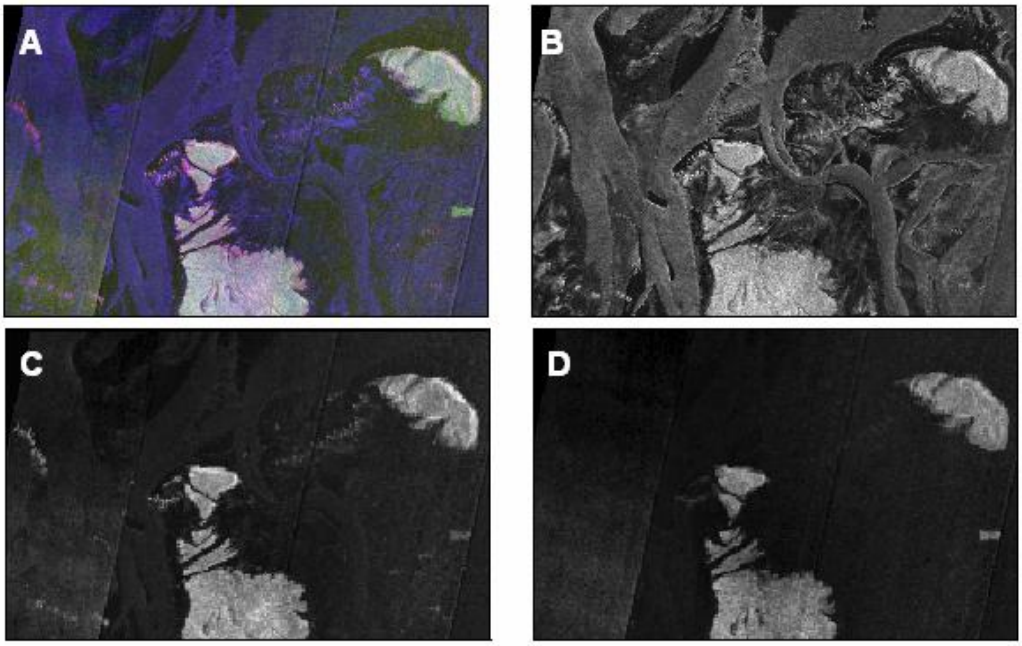

Figure 3. Area A - *SAR R99B image* for Taperaçu intertidal sandflat. A) RGB color composite (R-HH, G-HV, B-VV), B) VV, C) HH, D) HV.

Transverse vegetated dunes appear in magenta color in composite image (**Figure 4A**). Vegetated dunes produces a low radar return in comparison to the surrounded mangrove, with the better contrast in the HH- and VV-polarization images, respectively. The dark tones are related to absorptions of L-band in the dry sandy sediments, and the small backscattering must be related to geometric pattern of scrub vegetation. Paleo-dunes produce a high radar return in all of three-polarizations is response to salty grassland sandflat interaction, while in the flooded grassland interdunes VV-polarization presents a high radar return in relation to HH- and HV-polarization. This is explained by vertical orientation of grassland.

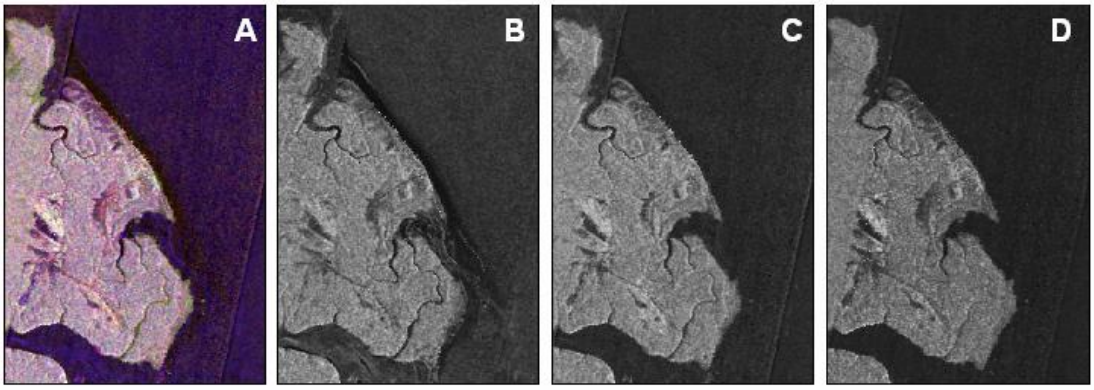

Figure 4. Area B - *SAR R99B image* for Ajuruteua macrotidal beach and coastal dunes. A) RGB color composite (R-HH, G-HV, B-VV), B) VV, C) HH, D) HV.

Intertidal Mangrove areas

They are located between the high spring tide and mean tidal level. Field studies have indicated that *Rhizophora* sp. and *Avicennia* sp. are the dominant species commonly found along this coast with 15 m to 20 m in height. About 20 years ago, a road was constructed, connecting the city of Bragança with the Ajuruteua beach (**Figure 1**). Following the death of mangrove vegetation by disturbances of the hydrological regime, this area was completely deforested. Currently, part of this degraded area shows an incipient natural regeneration (Souza Filho and Paradella, 2002).

The multi-polarized composite image reveals some strong contrast between different mangrove stage-healthful mangrove forest, regenerating mangrove and deforested area (**Figure 5**). Deforested mangrove areas present a low radar return in all three-polarizations, due to specular reflection of L-band over mudflat. In the regenerating mangrove area, HH-polarization presents the best contrast between all mangrove stages. Double-bounce scattering between trunks and ground is present for the younger trees. This certainly explains the high digital number (DN) value for regenerating mangrove areas. The absence of double-bounce over mature forest must be, principally related with tide condition during image acquisition (low spring tide). In VV-polarization some contrast can be observed, while in HV-polarization, regenerating mangrove areas is almost imperceptible. The healthful mangrove, as biomass increase, volume scattering dominates and the co-polarizations HH and VV show similar DN values and remain constant. In contrast, HV image presents lower DN values.

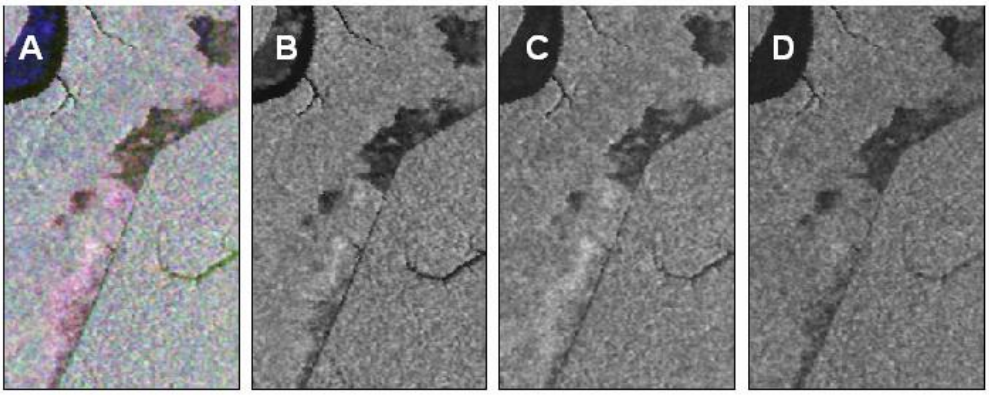

Figure 5. Area C - *SAR R99B image* for mangrove areas. A) RGB color composite (R-HH, G-HV, B-VV), B) VV, C) HH, D) HV.

Supratidal mangroves, marshes and coastal plateau – transitional zone

The salt marshes are known in the area as "Campos de Bragança". The marshes are situated in the supratidal zone; sedimentation is marked by mud deposition carried from tidal fluxes along creeks (Souza Filho and El-Robrini, 2000). The map in **Figure 1** shows the spatial relationship between salt marsh, old beach ridges and tidal mudflats.

A composite image and three-polarization amplitude images are shown in **Figure 6**. The composite image shows that the SAR R99B image is capable of mapping the transition between salt marshes and supratidal mangroves. It is possible to observe a strong contrast in the colors of multi-polarized composite image. The central magenta area indicates sources of scattering including crown components as well as trunk and ground surface present for the smaller scrub vegetation in the supratidal condition. Dark tones represent the specular reflection of L-band in all three-polarizations. The redish surrounding area is related to HH-polarization, whose scattering decrease continuosly with biomass rising in direction to intertidal mangrove areas (right side of the figures). The greatest variability in DN values

occurs in the HH-polarization, indicating that this polarization presents the best contrast between supra- and inter-tidal mangrove, followed by VV- and HV-polarization. In the other hand, HV-polarization is the best to distinguish the contact between mangrove and coastal plateau. The greenish area on the base of the figure indicates the dominance of cross-polarized return, which would be expected from volume or multiple scattering as the result of greater depolarization.

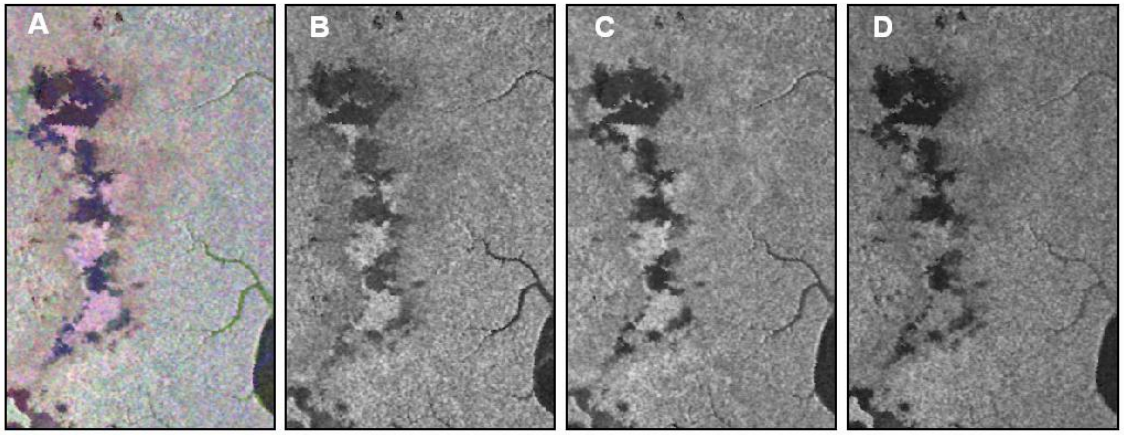

Figure 6. Area D - *SAR R99B image* for *Supratidal mangroves, salt marshes and coastal plateau- transitional zone*. A) RGB color composite (R-HH, G-HV, B-VV), B) VV, C) HH, D) HV.

The **Figure 7** shows a composite image and three-polarization amplitude images of the inner fresh marsh in contact with the coastal plateau. In all three-polarized images, fresh marshes appear as a very dark specular surface in response to a flooded area with emerged grassland. The boundary between fresh marsh and coastal plateau is perfect delineated.

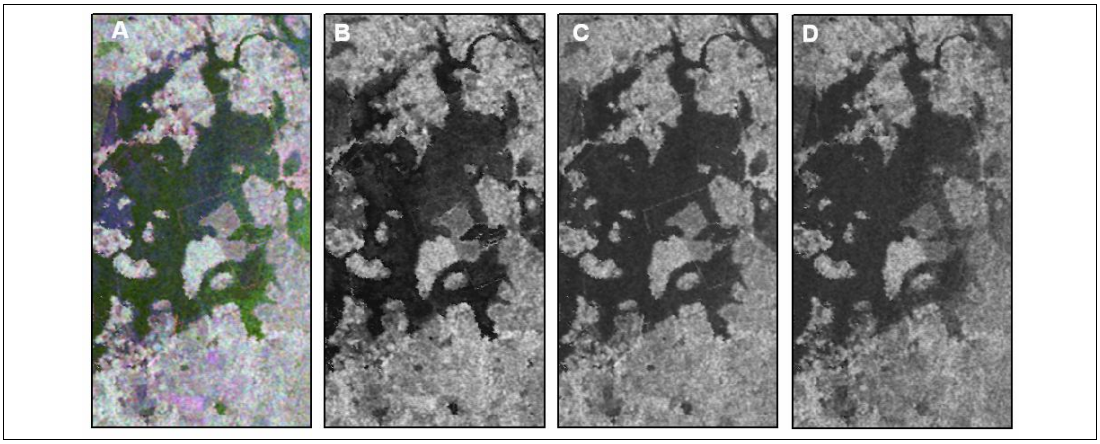

Figure 7. Area F - *SAR R99B image* for *fresh marshes and coastal plateau- transitional zone*. A) RGB color composite (R-HH, G-HV, B-VV), B) VV, C) HH, D) HV.

5. Conclusions

In this study was used multi-polarization L-band from SAR R99B image to investigate the usefulness of imaging radars for coastal wetland zone applications in the Amazon Region. High-resolution SAR R99B data can provide an excellent source for identification and delineation of geomorphic targets in the wetlands zones. Particularly, the VV-polarization was

the best polarization to recognize shallow water morphology in the intertidal zone. In relation to mangroves and marshes, HH-polarization showed the greatest variability in digital number (DN) values, followed by VV-polarization, indicating that their use is the best option to recognize and map these coastal environments. In addition to the enhanced target information, a preliminary analysis of multi-polarization images from different surfaces types indicates that the HH- and VV-polarization provide an excellent source for delineating transitional zones between different coastal environments.

Furthermore, observed differences between three-polarizations analyzed in this study were difficult to be interpreted. Future fieldwork has been planned to get a theoretical analysis of the observation, mainly after SAR R99B image calibration.

References

Costa, M.P.F.; Novo, E.M.L.M. ; Mantovani, J.E. Biophysical Properties and mapping of aquatic vegetation during the hydrological cycle of the Amazon floodplain using JERS-1 and RADARSAT. **International Journal of Remote Sensing**, v. 23, p. 1401-1426, 2002.

Hess, L.L. ; Melack, J.M. ; Simonette, D.S. Radar detection of flooding beneath the forest canopy. A review. **International Journal of Remote Sensing**, v. 5, p. 1313-1325, 1990.

Kasischke, E.S.; Melack ,J.M.; Dobson, M.D. The Use of Imaging Radars for Ecological Applications - A Review. **Remote Senssing of Environment**, v. 59, p. 141-156, 1997.

Mougin, E.; Proisy, C.; Marty, G.; Fromard, F.; Puig, H.; Betoulle, J. L.; Rudant, J. P. Multifrequency and Multipolarization Radar Backscattering from Mangrove Forests. **IEEE Ttransactions on Geoscience and Remote Sensing**, v. 37, p. 94-102, 1999.

Mura, J.C. ; Paradella, W.R. ; Dutra, L.V. ; Teruiya, R.K. **Metodologia da simulação de imagens MAPSAR a partir dos dados do sensor aerotransportado SAR-R99B do CENSIPAM**. São José dos Campos: Instituto Nacional de Pesquisas Espaciais, 2006. 9p (Internal Report).

Parmuchi, M.G.; Karszenbaum, H.; Kandus, P. Mapping wetlands using multi-temporal RADARSAT-1 data and a decision-based Classifier. **Canadian Journal of Remote Sensing**, v. 28, p. 175–186, 2002.

Pope, K.O.; Rejmankova,E.; Paris, J.; Woodruff. R.Detecting Seasonal Flooding Cycles in Marshes of the Yucatan Peninsula with S IR-C Polarimetric Radar Imagery. **Remote Senssing of Environment**, v. 59, p. 157-166, 1997.

Schröder, R.; Puls, J.; Hajnsek, I.; Jochim, F.; Neff, T.; Kono, J.; Paradella, W.R.; Quintino, M.M.; Valeriano, D.; Costa, M.P.F. MAPSAR: A small L-band SAR mission for land observation. **Acta Astronautica**, v.56, p. 35-43, 2005.

Souza Filho, P.W.M.; El-Robrini, M. Coastal Zone Geomorphology of the Bragança Area, Northeast of Amazon Region, Brazil. **Revista Brasileira de Geociências**, v. 30, p. 518-522, 2000.

Souza Filho, P.W.M.; Paradella, W.R., W.R. Recognition of the main geobotanical features along the Bragança mangrove coast (Brazilian Amazon Region) from Landsat TM and RADARSAT-1 data. **Wetlands Ecology and Management**, v. 10, p. 123-132, 2002.

Souza Filho, P.W.M.; Paradella, W.R. Use of RADARSAT-1 Fine and Landsat-5 TM selective principal component analysis for geomorphological mapping in a macrotidal mangrove coast, Amazon Region. **Canadian Journal of Remote Sensing**, v. 31, p. 214-224, 2005.

Souza Filho, P.W.M.; Martins, E.S.F.; Costa, F.R. Using mangroves as geological indicator of coastal changes in the Bragança macrotidal flat, Brazilian Amazon: an approach from remote sensing data and GIS. **Ocean & coastal management**, v. 49, p. 462-475, 2006.